Spinning dark matter halos promote bar formation

Kanak Saha[1][*] & Thorsten Naab[2]

[1] *Max-Planck-Institut für Extraterrestrische Physik, Giessenbachstrasse, D-85748 Garching, Germany*
[2] *Max-Planck Institut für Astrophysik, Karl-Schwarzschild Strae 1, 85748 Garching, Germany*

ABSTRACT

Stellar bars are the most common non-axisymmetric structures in galaxies and their impact on the evolution of disc galaxies at all cosmological times can be significant. Classical theory predicts that stellar discs are stabilized against bar formation if embedded in massive spheroidal dark matter halos. However, dark matter halos have been shown to facilitate the growth of bars through resonant gravitational interaction. Still, it remains unclear why some galaxies are barred and some are not. In this study, we demonstrate that co-rotating (i.e., in the same sense as the disc rotating) dark matter halos with spin parameters in the range of $0 \leqslant \lambda_{\rm dm} \leqslant 0.07$ - which are a definite prediction of modern cosmological models - promote the formation of bars and boxy bulges and therefore can play an important role in the formation of pseudobulges in a kinematically hot dark matter dominated disc galaxies. We find continuous trends for models with higher halo spins: bars form more rapidly, the forming slow bars are stronger, and the final bars are longer. After 2 Gyrs of evolution, the amplitude of the bar mode in a model with $\lambda_{\rm dm} = 0.05$ is a factor of ~ 6 times higher, $A_2/A_0 = 0.23$, than in the non-rotating halo model. After 5 Gyrs, the bar is ~ 2.5 times longer. The origin of this trend is that more rapidly spinning (co-rotating) halos provide a larger fraction of trailing dark matter particles that lag behind the disc bar and help growing the bar by taking away its angular momentum by resonant interactions. A counter-rotating halo suppresses the formation of a bar in our models. We discuss potential consequences for forming galaxies at high-redshift and present day low mass galaxies which have converted only a small fraction of their baryons into stars.

Key words: galaxies:halos – galaxies: spiral – galaxies: structure – galaxies: kinematics and dynamics – galaxies: evolution

1 INTRODUCTION

Optical and near-infrared observations indicate that nearly 2/3 of disc galaxies in the local universe are strongly barred (Eskridge et al. 2000; Grosbøl et al. 2004; Menéndez-Delmestre et al. 2007; Barazza et al. 2008). However, the fraction of barred disc galaxies might have significantly increased from high redshift until the present day. Whereas some studies indicate that it is nearly constant up to $z \sim 1$ (Jogee et al. 2004; Elmegreen et al. 2004; Marinova & Jogee 2007) other studies indicate a decrease in bar fraction towards higher redshift to values as low as 20% at $z \sim 0.84$ (Sheth et al. 2008). A common message from these observational studies is that bars can form in their

host stellar discs, embedded in diverse environments, and survive through $7 - 8$ Gyrs of look-back time. [1]

The formation mechanisms of a bar have been mostly studied with N-body simulations. They can either form as a result of swing-amplification of gravitationally unstable $m = 2$ modes in a stellar disc (Toomre 1964; Goldreich & Tremaine 1979; Toomre 1981; Combes & Sanders 1981; Sellwood & Wilkinson 1993; Polyachenko 2013), triggered by galaxy interactions and mergers (Noguchi 1987; Barnes & Hernquist 1991; Miwa & Noguchi 1998) or through the cooperation of orbital streams which eventually lead to formation of a bar (Earn & Lynden-Bell 1996). Interaction with dark matter halo substructures (Romano-Díaz et al. 2008) as well as the resonant gravitational interaction with the surrounding dark

---

[*] E-mail:saha@mpe.mpg.de

[1] Throughout the text, by co-rotating dark matter halo, we refer to a halo rotating in the same direction as the embedded disc and opposite for the counter-rotating case.

matter 'particles' has been shown to promote bar formation (Athanassoula 2002; Dubinski et al. 2009). Without interactions or in otherwise isolated environments, the formation and evolution of bars in disc galaxies strongly depends on the properties of the surrounding dark matter halo. It has been known for a long time that a dynamically hot halo component is required to stabilize an otherwise gravitationally unstable rotating self-gravitating disc against bar formation. According to Ostriker & Peebles (1973), a stellar disc will go bar unstable if the ratio of total rotational kinetic energy to the potential energy exceeds 0.14 ± 0.03. If the disc is embedded in a non-rotating dark matter halo, the potential energy increases and the disc is stabilized against bar formation (Hohl 1976). This finding was again confirmed by Efstathiou et al. (1982) and quantified in terms of observable parameters like disc scale length and circular velocity. However, a study by Athanassoula & Misiriotis (2002); Athanassoula (2003) indicated that strong bars can form in cold discs embedded in massive dark matter halos casting doubts on the general applicability of the above criteria (Athanassoula 2008).

Traditionally, the dark matter halo was treated as a rigid component which does not respond to the dynamics of the disc stars. However, 'live' dark matter halos enhance the growth of bars in model galaxies by resonant interactions of disc stars with halo 'particles' taking away the disc's angular momentum (Debattista & Sellwood 1998; Athanassoula 2002, 2003; Holley-Bockelmann et al. 2005; Weinberg & Katz 2007; Ceverino & Klypin 2007; Saha et al. 2012). The exchange of angular momentum between the disc and halo has been a subject of active research over the last two decades and our understanding of the bar instability has improved significantly.

Most studies focused on the formation of bars in kinematically cold discs (which easily form bars) embedded in close to spherical non-rotating dark matter halos. The evolution of systems, especially dynamically hot discs which might even be dark matter dominated was left unexplored, mainly because such systems were not expected to form bars at all. However, such systems exist. Low Surface Brightness (LSB) galaxies are generally isolated, without nearby companions and are dominated by dark matter at all radii (de Blok et al. 2001). The evolution of such galaxies is expected to depend entirely on internal processes and it remains unclear how their discs become bar unstable (Matthews & Gallagher 1997; Pohlen et al. 2003), as $\sim$ 30% of LSB galaxies reported in the sample of Matthews & Gallagher (1997) are barred. The study of Saha et al. (2013) indicates, that hot stellar discs inside a massive non-rotating halo are stable against the formation of strong bars; they can form only weak bars over several Gyrs. In this paper, we test the hypothesis that halo rotation - in accordance with standard cosmological models - can promote the formation of strong bars even in the presence of massive dark matter halos.

One of the definite predictions from large scale dark matter simulations with ΛCDM cosmological models is that dark matter halos acquire a certain amount of spin due to the cosmic shear and mergers (Steinmetz & Bartelmann 1995; Bullock et al. 2001; Vitvitska et al. 2002; Springel et al. 2005; Bett et al. 2007) and they are hardly non-rotating. Their spin distribution
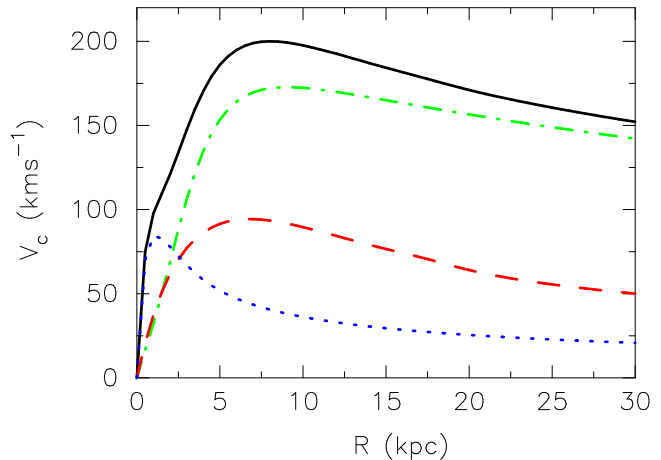

Figure 1. Circular velocity of disc stars (red dashed), bulge stars (blue dotted) and dark matter (green dot-dashed) of our fiducial initial condition galaxy. The galaxy disc dominated by dark matter (or a spheroidal bulge component) at all radii.

peaks at a value $\lambda_{\mathrm{dm}} \sim 0.035$ with a tail towards halos with even higher λ_{dm}-values. It has been suggested that rotating halos could enhance the growth of a bar (Weinberg 1985) as these halos have a higher fraction of dark matter particles on prograde orbits which can absorb disc angular momentum even more efficiently. We conduct a systematic investigation of the effect of halo spin on the evolution of a hot stellar disc embedded in a massive dark matter halo. The effect is tested with a galaxy model which is expected to be stable (or weakly unstable) against bar formation according to most of the conventional criteria of bar instability. We find that the spin of a dark matter halo has substantial effect on the bar instability and thereby on the galaxy evolution and carry out a detailed investigation using - cosmologically motivated - spinning dark matter halos.

The paper is organized as follows. Section 2 describes the construction of initial galaxy models with different halo spins and the basics of the simulation set up. Section 3 outlines different conventional criteria of bar instability. Bar evolution and the morphology of the disc is presented in section 4. Section 4.2 and section 4.3 discuss the effect of halo spin on the Ostriker-Peebles criteria and bulge formation respectively. Section 5 is devoted to angular momentum transfer and density wakes in the halo. Section 6 describes the resonances in the system. The discussion and conclusions are presented in section 7.

2 GALAXY MODELS WITH SPINNING HALO

We construct 5 equilibrium models of galaxy with initially spinning dark matter halos (hereafter, ISDM) using the self-consistent method of Kuijken & Dubinski (1995). Each galaxy model consists of a live disc, a dark matter halo, and a classical bulge. Flattened models of ISDMs are constructed by reversing the velocities of halo particles with negative angular momenta perpendicular to the disc plane, which remains a valid solution of the collisionless Boltzmann equation (Lynden-Bell 1962; Hernquist 1993; Saha & Gerhard 2013). In this way, we have constructed one model with a
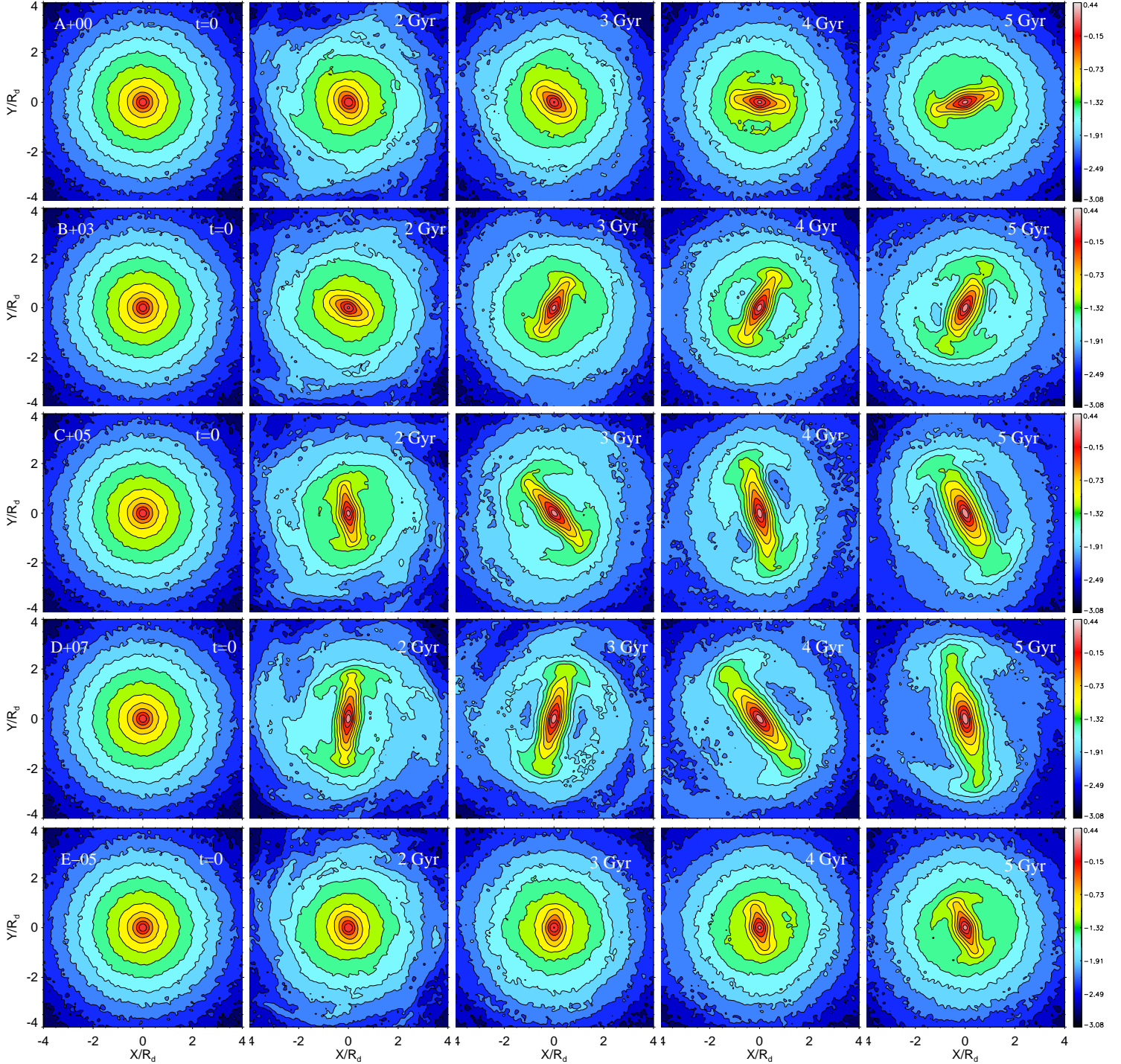
Figure 3. Time evolution (from left to right at t = 0, 2, 3, 4, 5 Gyrs) of the stellar surface density profiles for model with varying dark matter halo spins. From top to bottom the spin of the co-rotating (with the stellar disc) dark matter halos increases (models A+00, B+03, C+05, D+07). The bottom row shows the evolution of a model but with a counter-rotating halo (E-05). Models with more rapidly spinning co-rotating dark halos become bar unstable earlier and develop longer bars. Counter-rotating halos do not promote bar formation.

non-rotating halo (A+00), three models with co-rotating halos with spin parameters $\lambda_{\mathrm{dm}} \sim 0.03$, 0.05, and 0.07 (B+03, C+05, D+07) and one model with a counter-rotating halo (E-05) with a spin parameter of $\lambda_{\mathrm{dm}} \sim 0.05$, similar to model C+05 but the halo is rotating in the opposite direction of

the disc. For the definition of the spin parameter (λ_{dm}) of the dark matter halos we follow (Bullock et al. 2001),

$$\lambda_{\mathrm{dm}} \equiv \frac{1}{\sqrt{2}} \frac{\sum_i m_i \vec{r_i} \times \vec{v_i}}{M_{vir} V_{vir} R_{vir}}, \qquad (1)$$
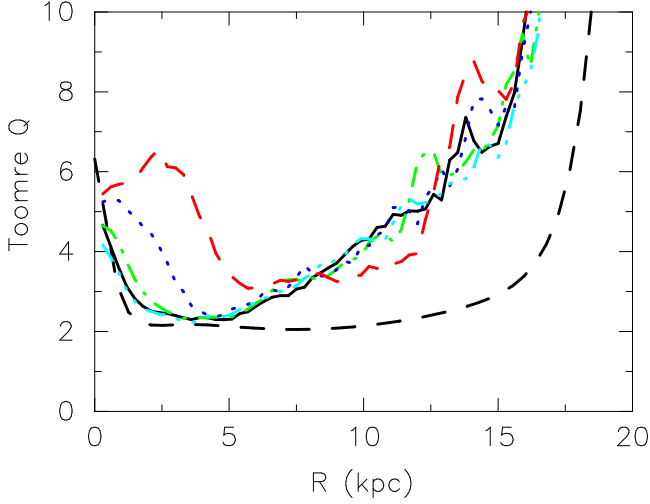
Figure 2. Radial profile of the Toomre Q parameter of the stellar disc. The dashed black line shows the initial condition at t=0. The other lines show the profiles after 2 Gyrs evolution for model A+00 (black solid), B+03 (green), C+05 (blue), D+07 (red), and the model with the counter-rotating halo E-05 (cyan). At any radius and at any time the stellar disc is stable in terms of Toomre $Q > 1$.

where m_i, $\vec{r_i}$ and $\vec{v_i}$ are the mass, radius and velocity of a dark matter particle; $V_{\mathrm{vir}}^2 = GM_{\mathrm{vir}}/R_{\mathrm{vir}}$ denotes the circular velocity at the virial radius (R_{vir}). The values of λ_{dm} are shown in Table 1 and reasonably cover the range of spin distributions of dark matter halos from cosmological simulations. An analysis of the Millennium simulation (Springel et al. 2005) indicates that the halo spin parameter only weakly depends on halo mass and shape (Bett et al. 2007). Therefore, we changed only the halo spin parameter keeping its mass and shape unchanged to single-out the effect of halo angular momentum on the disc evolution.

The disc has an exponentially declining surface density with a scale-length R_d, a constant scale-height h_z and mass M_d. The outer radius of the disc is truncated at $7.0R_d$ with a truncation width of $0.5R_d$ within which the stellar density smoothly drops to zero. The live dark matter halo is modelled with a distribution function given by the lowered Evans model (Evans 1993) which has a constant density core and produce a nearly flat rotation curve in the outer parts. The initial flattening of the halo is $q = 0.8$; the mass and tidal radius of the halo are given by $M_h = 10.32M_d$ and $R_h = 36R_d$ respectively. The preexisting classical bulge is represented by a King distribution function (King 1966). The mass and tidal radius of the bulge are $M_b = 0.18M_d$ and $R_b = 3.2R_d$ respectively. For relevant details on model construction, the reader is referred to Saha et al. (2010, 2012).

In terms of astronomical units, $M_d = 1.7 \times 10^{10} M_\odot$ and $R_d = 3.0$ kpc, so that the time unit is 24.0 Myr. The initial value of $h_z = 300$ pc. The total mass of the dark matter halo and the bulge is $M_h = 1.73 \times 10^{11} M_\odot$ and $M_b = 3.0 \times 10^9 M_\odot$, respectively. We use a total of 3.5×10^6 particles to simulate each model; assigning 1.2×10^6 to the disc, 1.8×10^6 to the halo, and 0.5×10^6 to the bulge. The softening lengths for the disc, bulge and halo are 9.0, 5.9 and 23.6 pc, respectively, following McMillan & Dehnen (2007). All simulations were performed using the Gadget
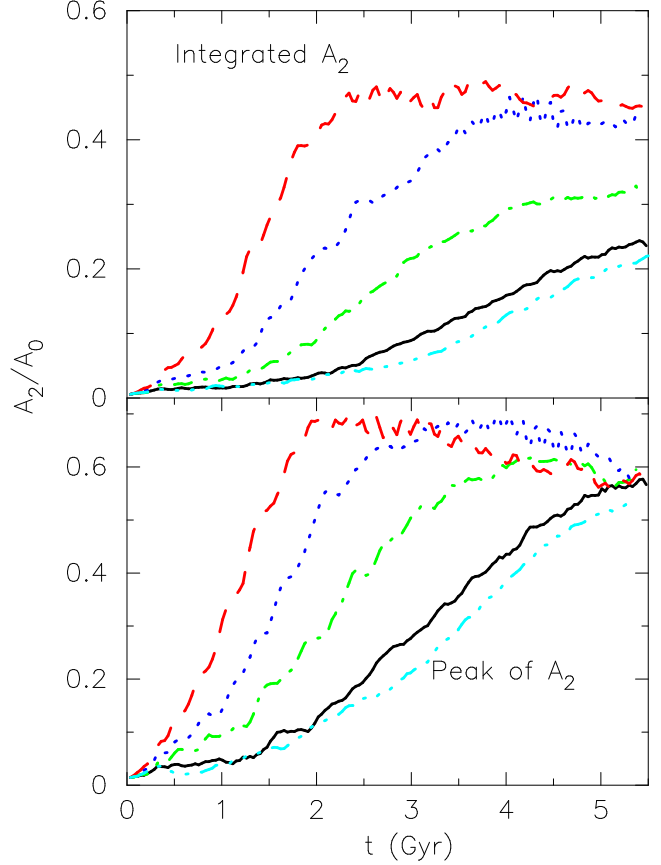

Figure 4. Time evolution of the peak of the $m = 2$ Fourier amplitude of the surface density. Red dashed line indicates D+07, blue dotted C+05, green dash-dot B+03, black solid line A+00, and cyan dash-dot-dot E-05. There is a clear trend for models with more rapidly spinning co-rotating halos to develop stronger bars at earlier evolutionary phases (e.g., D+07).
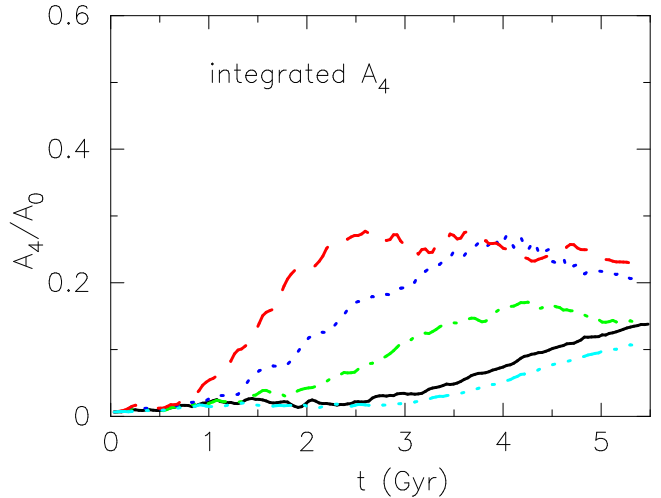

Figure 5. Same as in Fig. 4 but for the integrated $m = 4$ Fourier amplitude of the surface density.

Table 1. Initial spin of the dark matter halos, values of Ostriker-Peebles parameter and properties of bar at 5 Gyr. The unit of pattern speed Ω_B is in km s^{-1}kpc^{-1}.

Models	$\lambda_{\rm dm}$	$t_{\rm OP}$	$R_{\rm bar}/R_d$	$R_{\rm cr}/R_d$	Ω_B
A+00	0.000	0.039	1.32	3.28	18.3
B+03	0.032	0.053	1.61	3.91	15.0
C+05	0.053	0.078	1.78	4.72	12.2
D+07	0.074	0.115	2.60	4.76	12.0
E−05	-0.053	0.078	1.07	3.32	18.0

[2] $t_{\rm OP}$ denotes the Ostriker-Peebles criteria explained in section 3. $R_{\rm bar}$ is the bar size, $R_{\rm cr}$ the co-rotation radius and Ω_B is the bar pattern speed.

code (Springel et al. 2001) with an opening angle of $\theta = 0.7$ for the tree code performance and evolved all the models for about 5.5 Gyr. The half-mass rotation period (dynamical time-scale) at $2.5R_d$ is 237 Myr (37.75 Myr). At the end of the simulation the total energy was conserved to about $\sim 0.03\%$.

In Fig. 1, we show the circular velocity curve for the galaxy model constructed as described above. The model is dominated by dark matter (and a spheroidal bulge component) right from the central region, similar to some giant LSB galaxies (de Blok et al. 2001; Lelli et al. 2010). The initial stellar disc is kinematically hot and stable against local gravitational instability as can be seen from the initial radial profile of the Toomre Q (Toomre 1964) parameter (see Fig. 2), defined as $Q(R) = \sigma_r(R)\kappa(R)/3.36G\Sigma(R)$, where σ_r is the radial velocity dispersion, κ is the epicyclic frequency and Σ is the surface density of stars.

3   CRITERIA FOR BAR INSTABILITY

Many simulations have shown that a strong bar forms easily in a cold, rotation dominated stellar disc (Hohl 1971; Sellwood & Wilkinson 1993; Saha et al. 2012; Athanassoula 2012, and references therein). Based on the study of the stability of Maclaurin discs (Binney & Tremaine 1987) and N-body simulations of galactic discs, Ostriker & Peebles (1973) suggested that a stellar disc would become bar unstable if the ratio $t_{\rm OP} = T_{\rm rot}/|W|$ exceeds a critical value of 0.14 ± 0.03. In our simulations, we compute the Ostriker-Peebles criterion for each model in a slightly different way. Assuming the virial theorem applies to the isolated galaxy, it can be shown that (Binney & Tremaine 1987)

$$t_{\rm OP} = 1/(2 + T_{\rm rand}/T_{\rm mean}). \qquad (2)$$

$$T_{\rm rand} = \frac{1}{2}\int (v - \bar{v})^2 \rho(x)d^3x \qquad (3)$$

is the kinetic energy in random motions and

$$T_{\rm mean} = \frac{1}{2}\int \bar{v}^2 \rho(x)d^3x \qquad (4)$$

denotes the kinetic energy in the mean (primarily rotational) motion. To compute $t_{\rm OP}$ for each model galaxy, we need to add the contribution to the total kinetic energy budget from
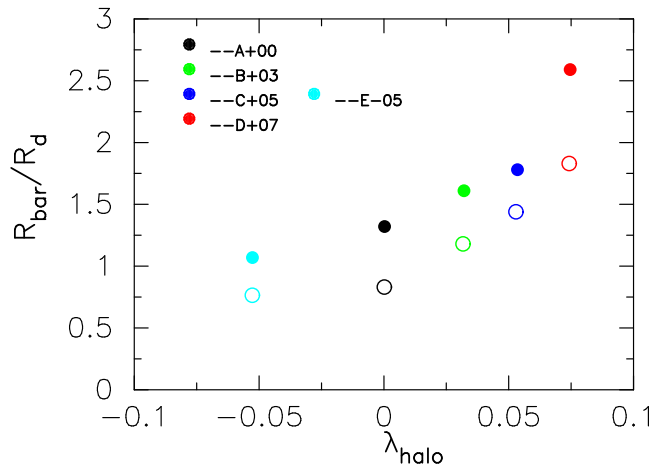

Figure 6. Bar size as a function of halo spin. Open circles indicate the sizes of the bars at $T = 3$ Gyr and filled circles at $T = 5$ Gyr. Open circle of a particular color refers to the same model as denoted by the filled circle of the same color. Bars in models with larger halo spin are larger at all times.
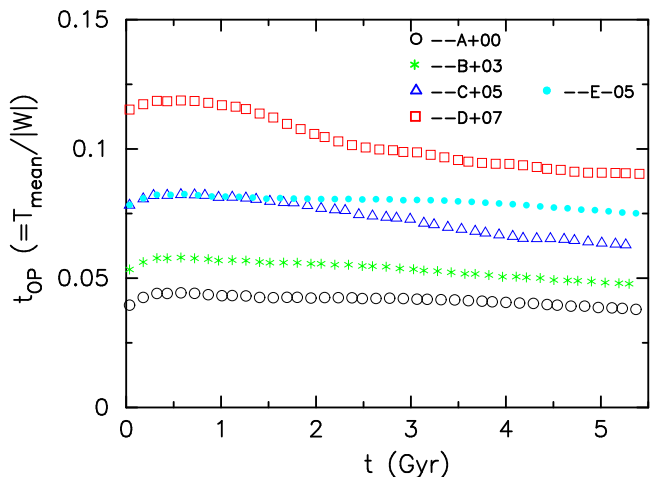

Figure 7. Time evolution of the Ostriker-Peebles stability parameter, $t_{\rm OP}$, (section 3) for models A+00 to E-05. According to this criterion all models should be stable against bar formation. However, this criterion accounts for the fact that the models with halo co-rotation are more prone to instabilities (e.g. higher values for $t_{\rm OP}$).

all the sub-components in the model e.g., bulge (B), disc (D) and halo (H), so that

$$T_{\rm rand} = T_{\rm rand,B} + T_{\rm rand,D} + T_{\rm rand,H}, \qquad (5)$$

and

$$T_{\rm mean} = T_{\rm mean,B} + T_{\rm mean,D} + T_{\rm mean,H}. \qquad (6)$$

Since the initial bulge and disc parameters are identical for all the models in our simulation, the variation in the initial $t_{\rm OP}$ arise due to the variation only in the halo spin. It is interesting to note that the total kinetic energy in a galaxy is independent of the sense in which particles are moving. So the total kinetic energy in a halo with a fixed spin parameter is the same, independent of whether it is co-rotating or counter-rotating with respect to the disc; $t_{\rm OP}$ is, however, sensitive to the net amount of halo rotation. It

is worth noting that D+07 has a higher value than other models and is likely to be unstable according to Ostriker-Peebles criteria. We will return to this issue in a later section.

A similar global criterion, suggested by Efstathiou et al. (1982), states that if $\alpha_{\rm eln} = V_{\rm peak}/\sqrt{GM_d/R_d} < 1.1$, a self-gravitating stellar disc would become bar unstable. Here, $V_{\rm peak}$ refers to the maximum of the rotational velocity. Basically, the dimensionless parameter $\alpha_{\rm eln}$ measures the ratio of the total mass within a given radius to that in the stellar disc, such that a massive halo would provide stability against bar formation. For a bare exponential disc without any bulge and dark halo, the value of $\alpha_{\rm eln} = 0.63$ (Efstathiou et al. 1982) and would be subject to vigorous bar instability. For our initial conditions $\alpha_{\rm eln} = 1.3$ indicating clearly that all the galaxy models would be stable against bar formation. Note that the value of $\alpha_{\rm eln}$ is insensitive to the halo rotation.

According to Toomre (1981) and a number of other studies (Sellwood & Wilkinson 1993; Dubinski et al. 2009, and references therein), bars in N-body simulations are formed through the swing-amplification mechanism. For this mechanism to work, the disc needs to have no inner Lindblad resonance (ILR), allowing the feedback loop to be in action. It has been shown that to achieve strong swing amplification of an $m = 2$ bar mode, a stellar disc requires to have $Q < 2$ and $1 < X_2 < 3$ (Julian & Toomre 1966; Toomre 1981). Here $X_2(R) = R\kappa^2(R)/(4\pi G\Sigma(R))$ is the swing-amplification parameter for an $m = 2$ mode in the tight winding approximation (Goldreich & Tremaine 1979). For the models considered here, the value of $X_2 = 6.4$ at $2.2R_d$ which marks the location of the peak of the disc's circular velocity. According to all classical stability criteria, the stellar discs in our simulation should be linearly stable (or weakly unstable) to strong bar formation.

4   BAR EVOLUTION - MORPHOLOGY

In Fig. 3, we show time evolution of the face-on surface density maps (from left to right) of the initially axisymmetric stellar disc embedded in a massive dark matter halo with different spin parameters (from top to bottom, see Table 1). The model with a non-rotating halo (A+00) remains nearly axisymmetric for about 2 Gyrs; however, as the spin of the halo increases, the disc starts forming a strong bar even earlier. It is clearly visible that the model with the strongest halo rotation (D+07) develops the strongest bar. The model with the counter-rotating halo (E-05) develops a bar in a similar way to the non-rotating model (A+00).

We have quantified this finding in Fig. 4 which shows the time evolution of the $m = 2$ Fourier component of the surface density normalized by the axisymmetric ($m = 0$) component, A_2/A_0 for all the models. In the lower panel of Fig. 4, we have shown the time evolution of the peak of the A_2/A_0 values – which is a valid definition of bar amplitude used frequently in literatures (Saha et al. 2010, 2013, and references therein). Till about ~ 3 Gyr, there is a clear correlation between bar amplitude and the halo spin – higher spin leads to higher A_2/A_0. However, beyond 3 Gyr, no such correlation is evident from the figure; while all the bar amplitudes nearly approaching to a single value at ~ 5 Gyr but with different bar sizes (see Fig. 3, section 4.1 and Table 1).

To avoid such intriguing situation, we compute the bar amplitude as integrated contribution of the $m = 2$ Fourier component over a radial range (which takes into account the radial variation of A_2/A_0 in the disc) as

$$\frac{\tilde{A}_2}{A_0} = \frac{1}{R_{\rm max}} \int_0^{R_{\rm max}} \frac{A_2}{A_0}(R)dR, \qquad (7)$$

where we chose $R_{\rm max} = 2.5R_d$, the region which confines most of the bars in our galaxy models at all times. The upper panel of Fig. 4, shows the integrated $\frac{\tilde{A}_2}{A_0}$ as a function of time. Within 3 Gyr, both methods give approximately same time variation for the bar amplitude, although they are quantitatively different. But after 3 Gyr, these two methods give entirely different result in that the integrated $\frac{\tilde{A}_2}{A_0}$ brings out the positive correlation with halo spin while the peak of A_2/A_0 does not. At about 2 Gyr, the integrated amplitude of the stellar bar in the halo with $\lambda_{dm} = 0.074$ is higher by a factor of ~ 11 compared to the non-rotating halo case. Both panels of Fig. 4 suggest that there is a clear trend – a more rapidly spinning co-rotating dark halo promotes the early formation of a strong bar.

From Fig. 3, a systematic increase in the bar length is noticeable as the spin of the co-rotating halo increases. A large-scale bar is formed in the model D+07 after 2 Gyr and by the end of the simulation at 5 Gyr the bar extends to ~ 8 kpc ($\sim$ the peak of the rotation curve, see Fig. 1). Interestingly, such a long and strong bar turns out to be a slow bar since it has formed and remain so throughout the simulation; as discussed, in detail, in section 6, all the bars in our simulations remain as slow bars at all times. Swing amplification (Toomre 1981) might have played an important role in the formation and growth of such a bar as our preliminary check showed no ILR (Inner Lindblad Resonances) which is crucial for establishing the feedback loop in the stellar disc. However, a detailed prediction of the initial bar pattern speed from most bar formation theories remains unclear. Note that in most models such bars do not trigger any two-armed spiral feature, except transient spirals; primarily because of the higher values of Toomre Q and X_2 parameter of the disc. As a bar grows, the combined effect of the bar and transient spirals heat the stars throughout the disc (Jenkins & Binney 1990; Saha et al. 2010) and as a result of that the Toomre Q of the disc rises to even higher values (see Fig. 2). This, in turn, reduces the possibility of growing spirals through swing amplification.

Interestingly, the growth of a stellar bar in our counter-rotating halo model (E-05) is significantly suppressed compared to the co-rotating model with the same spin (C+05). Substantial differences between C+05 and E-05 are clearly visible in the early phases of evolution (around 2 Gyr, Fig. 3). The evolution of E-05 is more similar to the model with the non-rotating halo (A+00).

In addition to a bar mode, the stellar discs in these models also develop higher order modes for which we restrict our analysis only to the $m = 4$ component. In Fig. 5, we show the time evolution of the $m = 4$ Fourier component of the disc surface density. It is apparent from the figure that $m = 4$ mode is significant in model D+07, the one with the highest halo spin in our sample. Not only a bar but also such an $m = 4$ component would take part in taking

away angular momentum from the stellar disc and thereby accelerate the overall transformation into a bar. The stellar discs of all 5 models do not grow any significant $m = 1$ mode (or higher-order odd modes).

4.1 Bar size and halo spin

After ~ 3 Gyr, all the models have grown a bar in their stellar discs. The size of a bar increases as time progresses by loosing angular momentum primarily to the dark matter halo. We compute the bar size in our model galaxies to understand its variation with the dark matter halo spin. There exists a number of ways to measure the size of a bar in a galaxy (Erwin 2005). In N-body simulations, the bar size measurements can be obtained from the radial profile of the $m = 2$ Fourier component ($A_2(r)$) and its phase angle variation with radius. We take the full width at half maximum (FWHM) of $A_2(r)$ as the first measurement of a bar size. Theoretically, the phase angle of a bar does not vary with radius but in reality, they do. We consider the radius at which the phase angle varies by $\sim 5°$ as the second measurement of the bar size. We take the mean of these two measurements to specify the bar size in our simulations. In Fig. 6, we show the bar size for the different models at two different epochs (after 3 Gyrs and 5 Gyrs). It is very clear that at a given time the bar has - at all epochs - significantly larger sizes for halos with larger spin parameters. The trend seems to be even non-linear. Note that in the case of a fast co-rotating halo, the bar size has increased by $\sim 50\%$ in 2 Gyrs.

4.2 Halo spin and the Ostriker-Peebles criterion

Ostriker & Peebles (1973) showed how an otherwise bar unstable stellar disc becomes more stable against bar formation as the mass of a surrounding dark halo increases. We show the time evolution of $t_{\rm OP}$ for our models in Fig. 7 (similar to Fig. 6 of Ostriker & Peebles (1973)). The initial value of $t_{\rm OP}$ for the model A+00 suggests that the disc should be stable against bar formation. Increasing the value of the halo spin (keeping its mass constant) makes the system more bar unstable and model D+07 has $t_{\rm OP} = 0.115$ and therefore should be marginally bar unstable. Indeed, this model develops the strongest early bar in our simulations which can be interpreted in the sense that the spin of the co-rotating halo increases the net rotational motion in the galaxy as a whole. However, other models (B+03 and C+05) also quickly develop bars and from our analysis we find that a hot stellar disc can become bar unstable within a reasonable time if $t_{OP} > 0.03$ which also happens to be the most probable spin parameter for a ΛCDM halo. However, in order to properly understand bar formation in galaxies, one needs to take into account the combined effect of the mass and spin (angular momentum) of the dark matter halo.

4.3 Bulge formation

Numerous N-body simulations have demonstrated that kinematically cold and thin stellar discs easily form bars that can transform into a central bulge-like structure, sometimes termed pseudo-bulges (see Kormendy & Kennicutt 2004, for
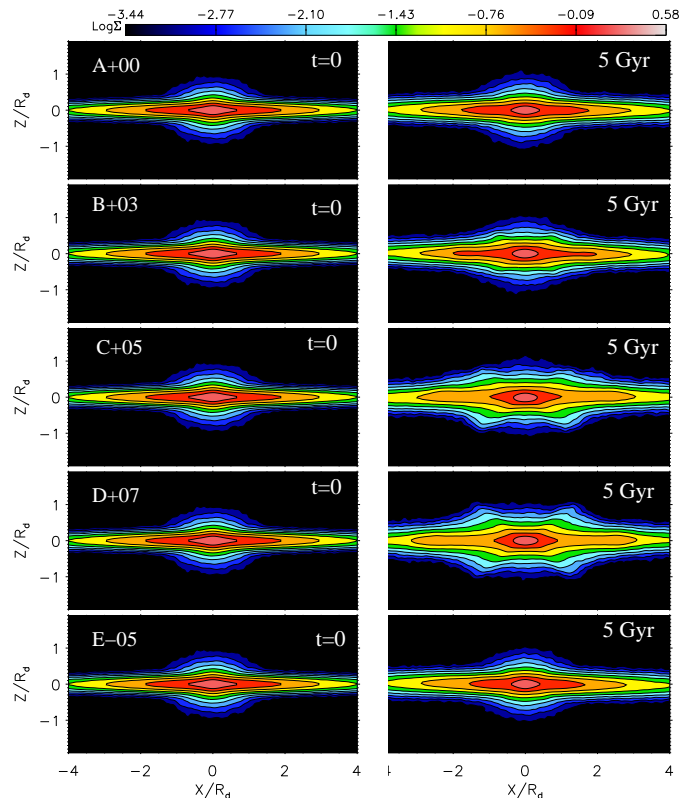

Figure 8. Edge-on galaxy morphology (stellar surface density) after 5 Gyrs of evolution (right) compared to the initial conditions (left). From top to bottom the spin of the dark matter halo increases; except for the bottom panel (counter-rotating halo model E-05). Spinning co-rotating dark matter halos promote the formation of peanut-shaped/boxy bulges (i.e. D+07).

a review). Boxy/peanut-shaped bulges are a class of bulges primarily formed via the buckling (or fire-hose) instability of a strong bar (Combes et al. 1990; Raha et al. 1991; Hernquist & Weinberg 1992; Athanassoula & Misiriotis 2002; Debattista et al. 2004; Kormendy & Kennicutt 2004; Saha et al. 2010, 2013). A detailed orbital analysis by Pfenniger & Friedli (1991); Patsis et al. (2002) shows that the presence of 2 : 1 and 4 : 1 vertical resonance plays an important role in the formation of such a boxy/peanut bulge. The time-scale to build such a bulge-like component in an isolated disc galaxy depends on various parameters such as the dark matter content, the value of Toomre Q in the disc, and might as well be influenced by a pre-existing 'classical' bulge (Saha et al. 2012). For kinematically cold discs ($Q \sim 1$), building a pseudo-bulge can take only one Gyr or less. In hot ($Q > 2$) and dark matter dominated discs, the time-scale to form a pseudo-bulge can be very long; in some cases it might even take a Hubble time (Saha et al. 2013).

In Fig. 8, we compare the final ($T = 5$ Gyrs) edge-on stellar morphologies (projected stellar surface density) of all galaxy models to the initial conditions ($T = 0$). The models with a non-rotating halo (A+00) and a counter-rotating halo (E-05) show bulge structures similar to the initial conditions, except for some amount of thickening due to heating by the weak bar (Saha et al. 2010). Although the stellar discs in both models (A+00 and E-05) form moderately strong bars
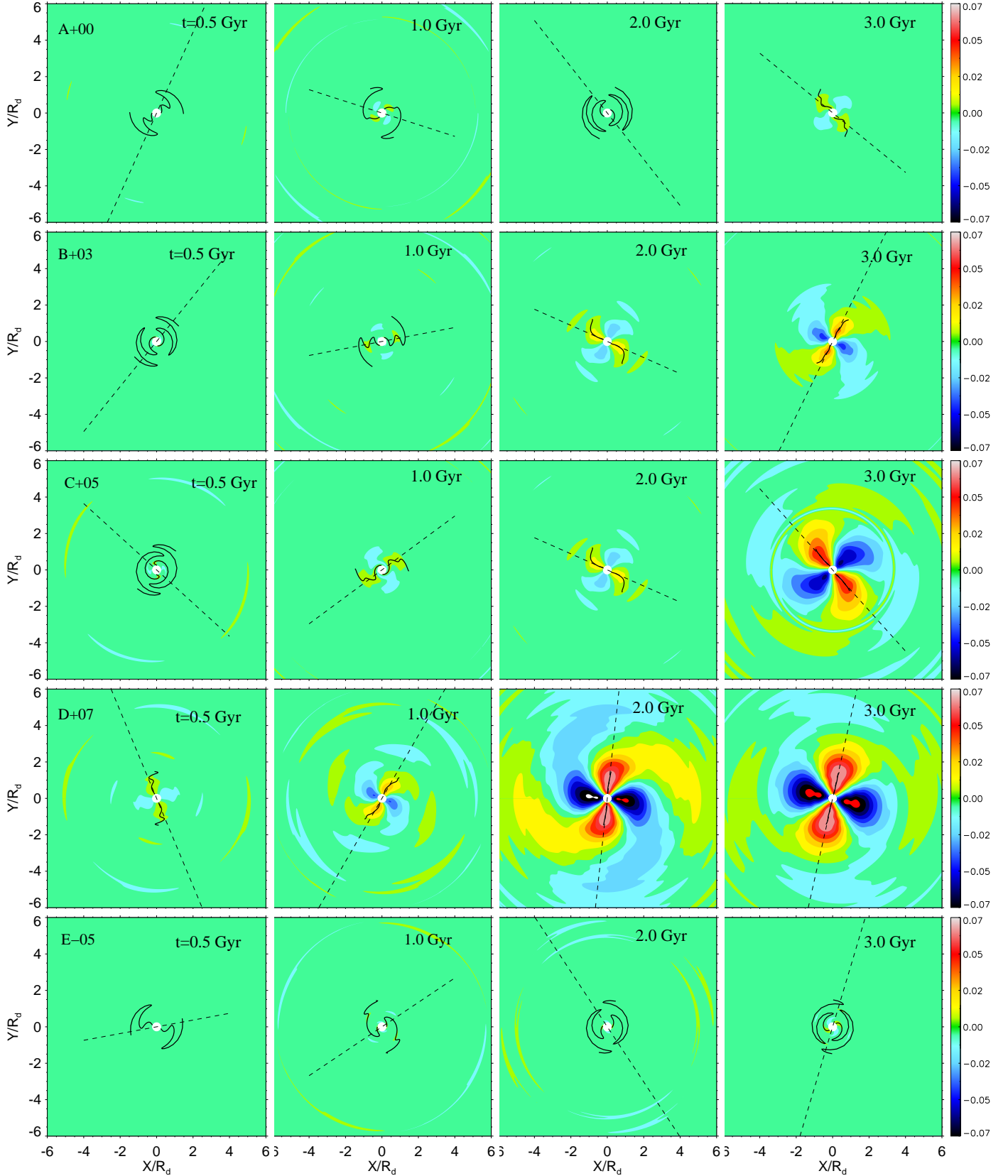
Figure 11. Time evolution (from left to right) of dark matter density wakes in the equatorial plane of the discs for models with varying halo rotation (from top to bottom). Red (blue) indicates over-dens (under-dens) regions with respect to the mean density at a given radius. The dashed line indicates the position angle of the stellar bar and the solid line follows the peak overdensity in the halo. The model with the highest halo spin (D+07) develops the strongest trailing density wakes in the halo (e.g., fourth row, second and third panel from the left). Trailing wakes result in angular momentum loss by dynamical friction.
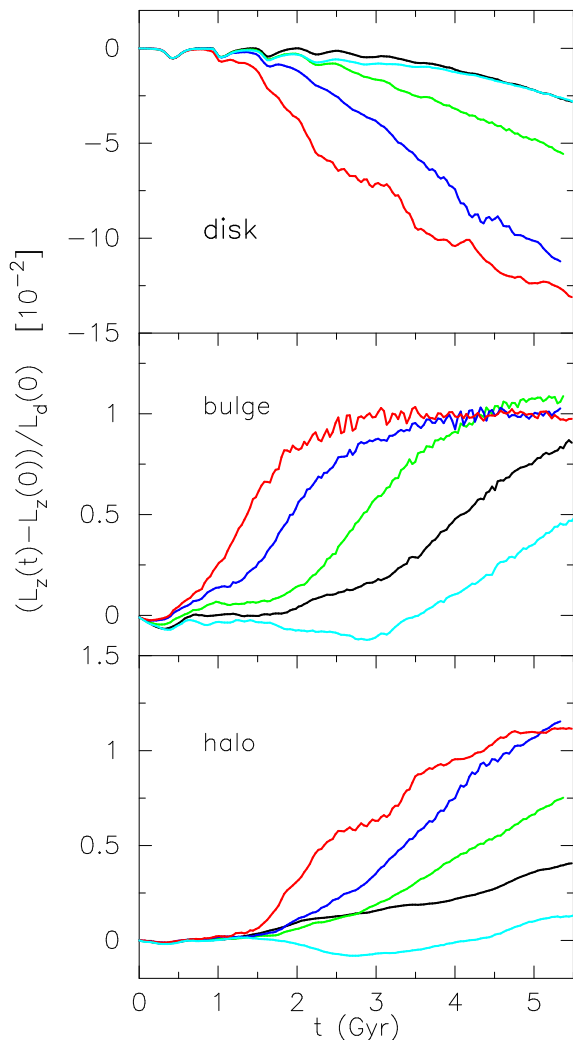
Figure 9. Time evolution of specific angular momentum of disc stars (upper panel), bulge stars (middle panel) and halo particles (bottom panel) for all 5 galaxy models. $L_d(0)$ denotes the disc specific angular momentum at $t = 0$. The red line denotes the model D+07, blue C+05, green B+03, black A+00, and cyan E-05. The mass of the halo is 57 times higher than that of the bulge. As expected the model developing the stronger bar transfers most angular momentum (D+07).

Figure 10. Time evolution of the pattern speeds of the bars, Ω_B, for all models. In models with more rapidly spinning halos the bar pattern speed is lower at late times.

at the end, they did not go through a buckling instability phase and have not developed a boxy/peanut-shaped bulge; see Saha et al. (2013) for a similar case in a dark matter dominated galaxy model. On the other hand, all models with a co-rotating halo develop bars that are strong enough to develop a buckling instability and form peanut-shaped/boxy bulges. The effect is strongest for the model with the highest dark matter spin (D+07). The buckling instability in this model occurred at around 3 Gyr - a corresponding drop in A_2 was not apparent from the lower panel of Fig. 4 as has been suggested in many previous works (Athanassoula 2012). But a mild drop in A_2 was seen when we used integrated A_2 (see upper panel of Fig. 4). Note that in a recent work by Saha et al. (2013), it has been suggested that the formation epoch of the boxy/peanut bulge is better correlated with the tilt of the velocity ellipsoid. The formation of boxy/peanut bulges not necessarily requires a fast and
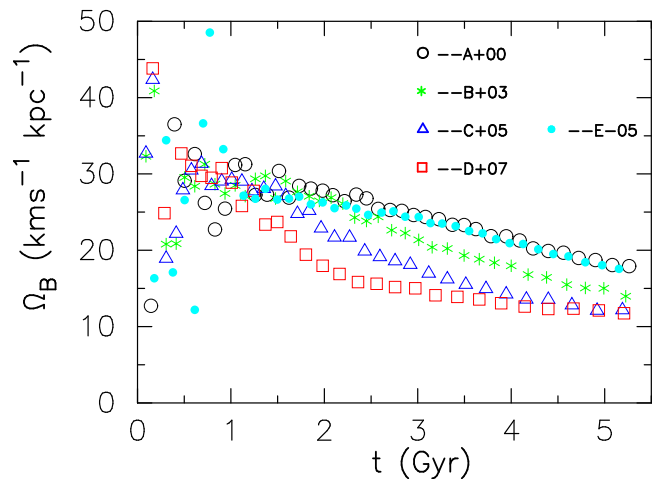
strong bar; they can form out of the slowly rotating bars as we have shown here. We compute the relative extent of the peanut length (see Fig. 8) with respect to the bar for the model D+07 following Saha & Gerhard (2013). We found that at $z = 0.4R_d$, the length of the peanut for this model at 5 Gyr is $\sim 60\%$ of the bar size (see Table 1). The orbital support for such a peanut bulge to form from a slowly rotating bars was found explicitly by Skokos et al. (2002) and their study could be relevant for a detailed understanding of the peanut bulges that form in our simulations (also for models A+00 and E-05 which did not form a peanut bulge). As the galaxy models in our simulations host pre-existing classical bulges, the models with halo spin develop composite bulges with a different origin and morphology. We emphasize here that knowing the mass model alone is not enough to understand the formation of a boxy/peanut bulge or composite bulge, one needs to have an access to the spin of the dark matter halo.

5 TRANSFER OF ANGULAR MOMENTUM AND DYNAMICAL FRICTION

Once a bar starts to form from disc stars, it grows via non-linear gravitational interactions involving the exchange of angular momentum with the outer parts of the disc, the surrounding dark matter halo and a pre-existing classical bulge (if present). The angular momentum is transferred by the gravitational torque produced by the bar (Lynden-Bell & Kalnajs 1972). Thereafter, it has been emphasized by several authors (Tremaine & Weinberg 1984; Weinberg 1985; Hernquist & Weinberg 1992; Weinberg & Katz 2002; Athanassoula 2002, 2003; Sellwood & Debattista 2006; Dubinski et al. 2009; Saha et al. 2012) that orbital resonances between disc stars and the particles representing the dark matter halos play a significant role in the transfer of angular momentum between the bar and the rest of the galaxy, with dark matter halo particles taking away most of the angular momentum from disc stars. In section 5.1 we discuss, in detail, the physical process that allows the

dark halo to do so. Most previous studies have investigated the transfer of angular momentum to a non-rotating dark matter halo. Here we quantify the angular momentum exchange between a bar and a rotating dark matter halo in more detail.

In Fig. 9, we show the time evolution of the specific angular momentum of the disc, bulge, and dark matter halo for all models. As mentioned above, the exchange of angular momentum between the stars and dark matter halo occurs when a resonant condition $l\kappa + n\Omega - m\Omega_B = 0$ between the bar and halo orbit is satisfied, Ω_B being the bar pattern speed. For the bar mode ($m = 2$), the important resonances are in this context $(l, n, m) = (-1, 2, 2)$ i.e., ILR; $(l, n, m) = (0, 2, 2)$ i.e., co-rotation. Independent of halo rotation, all stellar discs lose angular momentum which is deposited in the stellar bulge and the dark matter halo. The rate of angular momentum transfer correlates with the spin of the dark matter halo (or the strength of the bar). The amount of angular momentum transferred is highest in model D+07, qualitatively, in accordance with the semi-analytic results from Weinberg (1985). According to his calculation, the rate of angular momentum loss from the bar monotonically increases as the fraction of prograde orbits in the halo increases from 0 to 1. The reason for this is that prograde orbits contribute predominantly to the $(-1, 2, 2), (0, 2, 2)$ resonances which are, in general, stronger than $(-1, -2, 2), (0, -2, 2)$ resonances for a given l. For the same reason, one would expect less angular momentum transfer to a halo with a large fraction of retrograde orbits. In model E-05 with a counter-rotating halo, we see that the angular momentum loss from the stellar disc is nearly negligible up to ~ 3 Gyrs and only after 4 Gyrs it is comparable to the case of a non-rotating halo. Interestingly, the counter-rotating halo looses angular momentum between $\sim 1.5 - 4$ Gyrs of evolution. Only for model D+07 there is an indication that the angular momentum transfer to the halo might saturate.

As a result of the angular momentum loss from disc stars, the pattern speed of the bars decreases (Fig. 10). Models with stronger bars (more rapidly spinning dark matter halos) show a more rapid slowdown of the bar in accordance with (Weinberg 1985). The effect of halo rotation on the dynamical friction and hence the slow down of bar pattern speed was previously studied by Athanassoula (1996); Debattista & Sellwood (2000) while the former found the bar pattern speed to be decreasing rather slowly in a co-rotating halo. The bar in the model with the fastest rotating halo (D+07) slows down faster during the initial phase of evolution; the pattern speed of the bar in D+07 is nearly half of that in A+00 (non-rotating halo) at ~ 2 Gyr. Non-linear effects are also apparent from this figure. In model D+07, the pattern speed of the bar remains nearly unchanged from ~ 2.5 Gyr onwards although the halo keeps absorbing angular momentum (see Fig. 9). Since the bar in this model keeps growing, we think most of the angular momentum loss is likely to be invested into changing the moment of inertia of the bar according to:

$$\frac{dL_z}{dt} = I_B \frac{d\Omega_B}{dt} + \Omega_B \frac{dI_B}{dt}, \qquad (8)$$

where I_B and Ω_B are the moment-of-inertia and pattern

speed of the bar. Notice also that the angular momentum gain by the pre-existing classical bulge (in model D+07) nearly saturates beyond ~ 2.5 Gyr - a fact that correlates well with bar pattern speed slow down beyond ~ 2.5 Gyr in the same model. The pre-existing classical bulge is constructed with a streaming fraction of 0.5 i.e., half of the bulge stars are in retrograde orbits. Fig. 9 shows that the bulge stars initially looses angular momentum as in the counter-rotating halo model. Also all the bulges seem to be absorbing angular momentum earlier than the halo in our models. A detailed analysis of these findings is beyond the scope and aim of this paper and will be followed up using orbital analysis in a future paper. Overall, we find that a co-rotating halo with a reasonable spin parameter is capable of absorbing a significant amount of angular momentum from the disc (due to the formation of a stronger bar). As a result the bar can be slowed down by factor of 2 within about a Gyr, i.e. about 27 dynamical time scale computed at the half-mass radius after its formation.

5.1 Density wakes and the dark bar

A rotating self-gravitating bar inside a live dark matter halo will create a density wake in the halo density distribution that in turn exerts a torque on the bar and slows it down. This phenomenon is known as dynamical friction (Chandrasekhar 1943; Tremaine & Weinberg 1984) and has been studied, in great detail, by several authors, especially in the context of bar-halo friction (Weinberg 1985; Debattista & Sellwood 2000; Holley-Bockelmann et al. 2005; Sellwood & Debattista 2006; Weinberg & Katz 2007). Previous investigations of the bar-halo friction using N-body simulations, however, considered only non-rotating halos. In the following, we study the nature of density wakes in models with rotating halos in more detail.

We decompose the density distribution of the dark matter halos in different models into spherical harmonics $\rho_h(r, \theta, \varphi) = \rho_{lm}(r) Y_{lm}(\theta, \varphi)$. The density component ρ_{22} corresponding to $l = 2, m = 2$ is the strongest, although the contributions from $l = 4, m = 2$ and $l = 4, m = 4$ are non-negligible, especially in models D+07 and C+05. In Fig. 11, we show the density distribution ρ_{22} projected onto the equatorial plane ($\theta = 90°$) for each model at different times. In model A+00 (top row), we see a tiny bar-like density wake produced at about 3 Gyr. By the same time the density distribution of the counter-rotating halo model (E-05) remains nearly featureless without any density wakes . In contrast, strong bar-like density wakes are produced in all models with co-rotating halos; with increasing intensity as the spin parameter increases. The nature of the density wakes can be followed clearly in model D+07 (fourth row in Fig. 11). In the initial phase (less than ~ 2 Gyr), dark matter particles corresponding to the $l = 2, m = 2$ density wakes form a spiral-like structure which lags behind the bar in the stellar disc. The phase angle of the spiral-like structure with respect to the stellar bar varies with radius. As time progresses, the density wakes get stronger and forms a bar-like feature in the inner part with a nearly constant phase out to ~ 2 disc scale lengths. At larger radii the wakes still have a spiral-like structure and lag behind the stellar bar. The swarm of dark matter particles in the spiral-like wakes lagging behind the stellar bar are the primary source
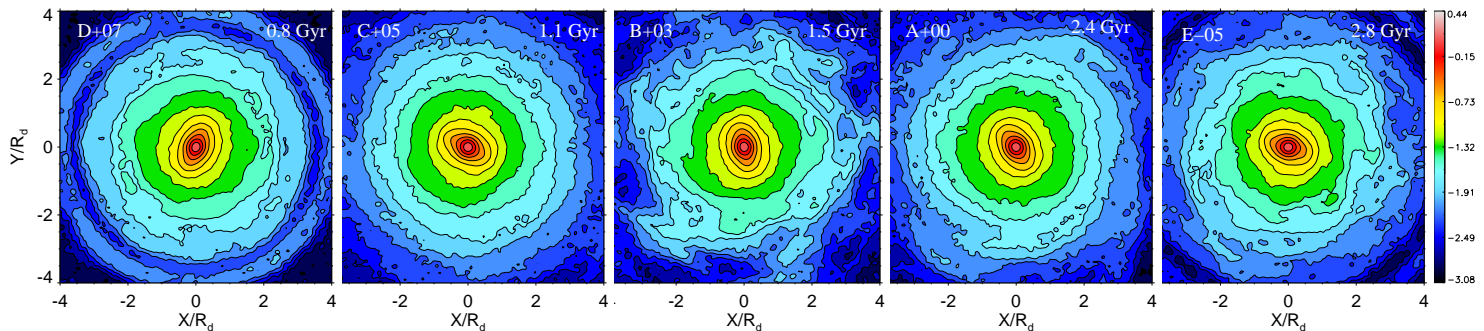
Figure 12. Surface density of stars of each model galaxy shown at the time when the bar has just formed. Formation times are given in the upper right corner of each panel. The bar forms first (after 0.8 Gyrs) in the model with the highest halo spin (D+07, left) and last (after 2.8 Gyrs) in the model with the counter-rotating halo (F-05,right).
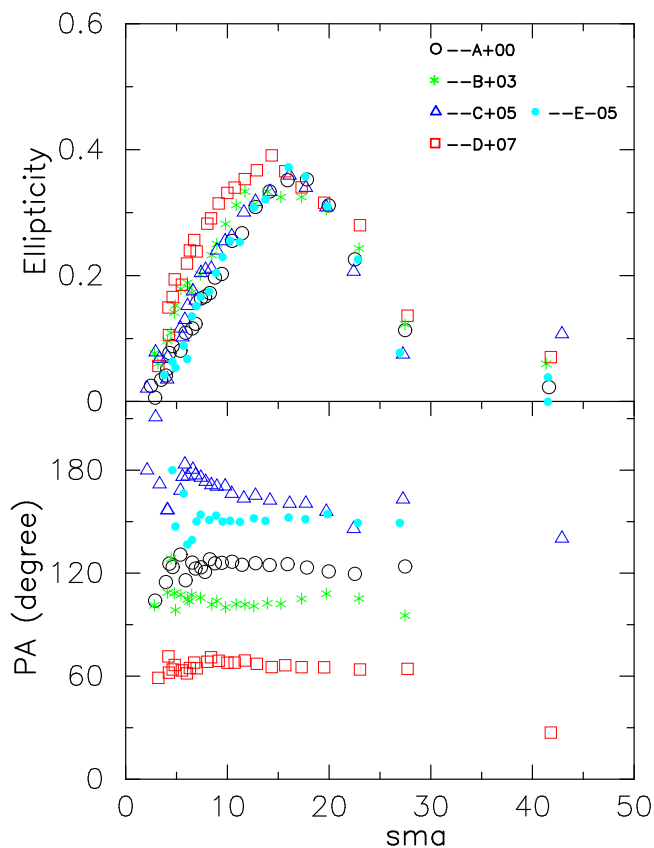

Figure 13. Ellipticity and position angles (PA) as a function of the semi-major axis of the bars at the time of their formation (see Fig. 12). All bars have similar ellipticity profiles but different position angles and pattern speeds (see Fig. 10). One sma unit corresponds to $0.04R_d$.

of dynamical friction. They exert torques on the bar and slow it down. At around 3 Gyr the spiral-like structure in model D+07 disappears, leaving behind a bar-like structure which is almost in co-rotation with the stellar bar. This feature has been called a dark bar or halo bar in the literature (Holley-Bockelmann et al. 2005; Athanassoula 2007). This dark bar is a resonance driven feature and would be hard to distinguish from the stellar bar as it has nearly the same pattern speed. The same happens in all other models

with co-rotating halos, however less rapidly for halos with lower spin parameters.

6 RESONANCES AND SLOW BARS

To understand the nature and dynamics of the bars forming in models with spinning halos, we identify the birth time of the bars by inspecting the maximum values of A_2/A_0, the radial variation of the projected ellipticity and the position angle of the semi-major axis of the bars. As explained above, dark matter halos with high spin parameter promote the early formation of bars, which is quantified here. In Fig. 12, we show the face-on stellar surface density maps for all models at the corresponding birth time of the bars which we have defined in the following way: a bar is 'born' when the peak ellipticity (ϵ_{max}) along the bar semi-major axis becomes larger than 0.3, and the the corresponding PA is almost constant. In Fig. 13, we show the ellipticity and the position angle as a function of the semi-major axis (sma). The aforementioned range of the peak ellipticity roughly corresponds to $(A_2/A_0)_{max} \sim 0.2$ (see Fig. 4). At formation, all bars have very similar shapes but they have different pattern speeds. We compute the size of the nascent bar using only the radial variation of its PA in the same way as explained in section 4.1. This way, we get the largest size of the bar, called as L_{bar} in the literature (e.g. Erwin 2005), in all models and the corresponding values are given in Table 2. We use the estimate of L_{bar} to get a lower limit on the ratio of the co-rotation radius to the radial extent of the bar, R_{cr}/R_{bar}, which decides whether these initial bars are slow or fast in nature. A bar is termed 'fast' if $1.0 < R_{cr}/R_{bar} < 1.4$ and 'slow' for which the ratio is greater than 1.4 (Aguerri et al. 2003).

Next, we calculate the locations of the resonances in the stellar disc to see whether spinning halos preferentially create slow bars. Observations and simulations (without halo rotation) by Chemin & Hernandez (2009) already indicated that systems dominated by dark matter can only develop slow bars. Fig. 14 shows the location of co-rotation resonances when the bar has just formed in the disc and towards the end of the simulation. We have checked that there was no ILR in the stellar disc initially. From Fig. 10, we know that the nascent bar in model D+07 rotates faster than all others (open red circle in Fig. 14) with CR at ~ 6 kpc. The slowest

Table 2. Properties of nascent bars. The unit of pattern speed Ω_B is in km s^{-1}kpc^{-1}.

Models	L_{bar}/R_d	Ω_{B}	R_{cr}/R_d	$R_{\mathrm{cr}}/L_{\mathrm{bar}}$
A+00	0.85	26.9	2.20	2.58
B+03	0.90	27.0	2.18	2.42
C+05	0.72	29.0	2.00	2.77
D+07	1.10	29.5	1.95	1.77
E-05	0.80	24.5	2.50	3.12

[3] L_{bar} is the length of the bar measured based on the phase angle variation. Rest of the symbols are explained in Table 1.
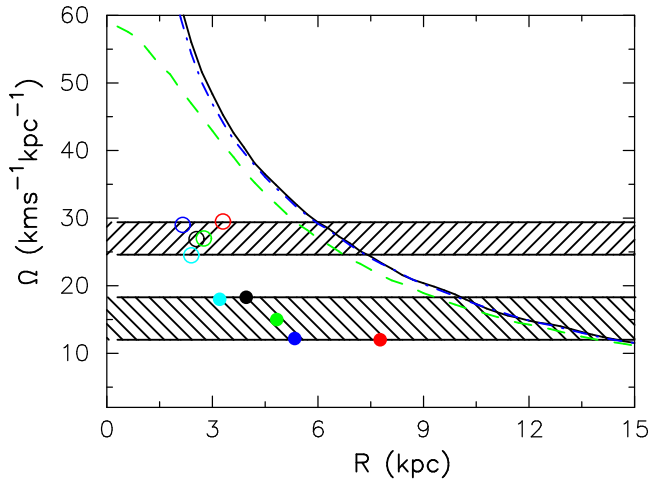
Figure 14. Location of co-rotation resonances in the stellar disc which has just formed a bar and at a later time, 5 Gyr. The forward hatched region denotes the range of pattern speeds amongst the nascent bars (at the time of their formation, see Fig. 12) and the back-hatched region for the evolved bars at 5 Gyr. The ranges of pattern speeds are given in Table 1 and Table 2. The solid black and dashed green curves refer to Ω for D+07 at those two instances and dash-dot curve for the model A+00 at 5 Gyr. Open circles refer to the sizes and pattern speeds of the nascent bars while filled circles are those of the evolved bars. The colors are identical to previous figures.

rotating bar in model E-05 (couter-rotating halo, open cyan circle) pushes CR to $\sim$ 7.5 kpc. Comparing, the bar sizes and CR radii we find that $1.77 < R_{cr}/R_{bar} < 3.1$ which is larger than 1.4 for all models, i.e. above the limit for fast bars. This property does not change with time. After 5 Gyrs of evolution the bars are in the range $1.83 < R_{cr}/R_{bar} < 3.1$. The values for bar sizes, CR radii and pattern speeds after 5 Gyrs are quoted in Table 1.

We conclude that all bars in the galaxy models presented here form as slow bars and they remain slow bars as the galaxy evolves. The transformation of a slow bar to fast is unlikely. Increasing the spin of a halo (to more unlikely values) could possibly reduce the ratio R_{cr}/R_{bar} close to 1.4 leading to the possibility of harboring a fast bar in a dark matter dominated galaxy. It is worthwhile to point out that bars in early-type galaxies are generally fast, while they could either be slow or fast in late-type galaxies (Aguerri et al. 2003; Rautiainen et al. 2005).

7 SUMMARY AND DISCUSSION

In this paper we have demonstrated that spinning dark matter halos promote the formation of stellar bars, the most common and most intriguing non-axisymmetric feature in galaxies. Even dark matter dominated hot stellar discs, which are expected to be stable against bar formation according to traditional criteria (see e.g., Ostriker & Peebles 1973; Efstathiou et al. 1982, however, see Athanassoula 2008) , can form strong bars depending on the spin of their co-rotating host halos. Stellar discs embedded in faster spinning halos - we have tested halos in the range $0 < \lambda_{\mathrm{dm}} < 0.07$ - develop their bars up to 2 Gyrs earlier with a higher ($m = 2$) Fourier amplitude (up to peak $A_2/A_0 \sim 0.7$) and the final bars are longer (up to a factor of 2.5). The essence of effect has been suggested by (Weinberg 1985) and is caused by more efficient angular momentum transfer from the disc to the spinning dark matter halos due to resonant interactions between disc stars and co-rotating halo particles. We have demonstrated that dynamical friction between a bar and a halo is stronger when the halo is co-rotating with the disc leading to significant transfer of angular momentum to the dark matter particles which form a bar-like structure in the inner region. As a result, a higher local density of dark matter particles can be expected wherever the stellar bar is located. This effect is weakest in counter-rotating halos (we have tested one model) which thus appear to suppress the formation of bars. The presence of counter-rotating halos could plausibly explain why some of the observed massive and cold stellar discs did not form any bar at all (Sheth et al. 2012).

The dynamical friction between a rotating bar and spinning halo requires that the halo is composed of particles not just a rotating potential. Hence the effect would be visible when the dark matter halo is live i.e., is able to interact with the disk stars. In other words, rigid halos might not show the same dramatic effect.

Not all bars in our models form boxy/peanut-shaped (pseudo-) bulges in the end (Kormendy & Kennicutt 2004; Athanassoula 2005). Although the $m = 2$ peak amplitudes of all the bars are nearly the same after 5 Gyr, only the discs embedded in co-rotating halos with spin parameters $\lambda_{\mathrm{dm}} > 0.03$ went through a buckling instability phase. Discs embedded in faster spinning halos develop stronger bars and appear more box-shaped in the end.

The impact of halo spin on bar formation in the idealized model discs discussed here is unambiguous and might have important consequences for the formation and evolution of disc galaxies in ΛCDM cosmologies. As discussed in section 1, the rotation of dark matter halos is a definite prediction from large scale dark matter simulations with ΛCDM cosmological models (Steinmetz & Bartelmann 1995; Bullock et al. 2001; Vitvitska et al. 2002; Springel et al. 2005; Bett et al. 2007). As most of the stellar discs are expected to co-rotate with their host halos (see e.g., Sales et al. 2012; Aumer & White 2013), the formation of bars might be promoted in general. It has been shown by a number of studies that systems with already massive and dynamically cold stellar discs become bar unstable easily (Combes & Sanders 1981; Valenzuela & Klypin 2003; Dubinski et al. 2009; Sellwood & Debattista 2009;

Saha et al. 2012; Athanassoula et al. 2013) and a rotating halo might only accelerate the instability in those systems.

More interesting is the effect on systems which traditionally were not expected to be bar unstable but are observed to have bars. In particular, present day low-mass galaxies which are, in general, observed to be dark matter dominated (Barazza et al. 2008; Sheth et al. 2008; Chemin & Hernandez 2009; Nair & Abraham 2010) and - in the ΛCDM framework - are expected to have converted only a very small fraction of the available baryons into stars (Yang et al. 2012; Moster et al. 2013; Behroozi et al. 2012). Another class of galaxies for which the above effect might be very relevant are low surface brightness galaxies (LSB). They are dark matter dominated, their stellar discs are relatively hot at a very low level of star formation despite having a similar amount of gas as in their high surface brightness (HSB) counterparts. LSB galaxies are generally found in isolated environments which excludes the possibility of strong tidal interaction yet bars are found in these galaxies (Matthews & Gallagher 1997; Pohlen et al. 2003). Previous N-body simulations by (Mayer & Wadsley 2004) showed that LSB stellar discs embedded in CDM halos are generally stable against bar formation. Our study with spinning halos sheds new light on the prospect of bar formation in LSB galaxies.

Another interesting (but definitely more speculative) regime for this process to become important is at high redshift ($z > 2$) where star forming galaxies have hot disc components (Förster Schreiber et al. 2009) and a significant fraction of the baryons is still in the form of gas (Tacconi et al. 2012). Here rotating halos might promote the early and rapid formation of bars with important consequences for instability driven bulge evolution models (Genzel et al. 2008) and, eventually, the formation and early growth of supermassive black holes (Bower et al. 2006; Fanidakis et al. 2012; Hirschmann et al. 2012).

ACKNOWLEDGEMENT

REFERENCES

Aguerri J. A. L., Debattista V. P., Corsini E. M., 2003, MNRAS, 338, 465
Athanassoula E., 1996, in Buta R., Crocker D. A., Elmegreen B. G., eds, IAU Colloq. 157: Barred Galaxies Vol. 91 of Astronomical Society of the Pacific Conference Series, Evolution of Bars in Isolated and in Interacting Disk Galaxies. p. 309
Athanassoula E., 2002, ApJ, 569, L83
Athanassoula E., 2003, MNRAS, 341, 1179
Athanassoula E., 2005, MNRAS, 358, 1477
Athanassoula E., 2007, MNRAS, 377, 1569
Athanassoula E., 2008, MNRAS, 390, L69
Athanassoula E., 2012, ArXiv e-prints
Athanassoula E., Machado R. E. G., Rodionov S. A., 2013, MNRAS, 429, 1949
Athanassoula E., Misiriotis A., 2002, MNRAS, 330, 35
Aumer M., White S. D. M., 2013, MNRAS, 428, 1055
Barazza F. D., Jogee S., Marinova I., 2008, ApJ, 675, 1194
Barnes J. E., Hernquist L. E., 1991, ApJ, 370, L65
Behroozi P. S., Wechsler R. H., Conroy C., 2012, ArXiv e-prints
Bett P., Eke V., Frenk C. S., Jenkins A., Helly J., Navarro J., 2007, MNRAS, 376, 215
Binney J., Tremaine S., 1987, Galactic dynamics
Bower R. G., Benson A. J., Malbon R., Helly J. C., Frenk C. S., Baugh C. M., Cole S., Lacey C. G., 2006, MNRAS, 370, 645
Bullock J. S., Dekel A., Kolatt T. S., Kravtsov A. V., Klypin A. A., Porciani C., Primack J. R., 2001, ApJ, 555, 240
Ceverino D., Klypin A., 2007, MNRAS, 379, 1155
Chandrasekhar S., 1943, ApJ, 97, 255
Chemin L., Hernandez O., 2009, A&A, 499, L25
Combes F., Debbasch F., Friedli D., Pfenniger D., 1990, A&A, 233, 82
Combes F., Sanders R. H., 1981, A&A, 96, 164
de Blok W. J. G., McGaugh S. S., Bosma A., Rubin V. C., 2001, ApJ, 552, L23
Debattista V. P., Carollo C. M., Mayer L., Moore B., 2004, ApJ, 604, L93
Debattista V. P., Sellwood J. A., 1998, ApJ, 493, L5
Debattista V. P., Sellwood J. A., 2000, ApJ, 543, 704
Dubinski J., Berentzen I., Shlosman I., 2009, ApJ, 697, 293
Earn D. J. D., Lynden-Bell D., 1996, MNRAS, 278, 395
Efstathiou G., Lake G., Negroponte J., 1982, MNRAS, 199, 1069
Elmegreen B. G., Elmegreen D. M., Hirst A. C., 2004, ApJ, 612, 191
Erwin P., 2005, MNRAS, 364, 283
Eskridge P. B., Frogel J. A., Pogge R. W., Quillen A. C., Davies R. L., DePoy D. L., Houdashelt M. L., Kuchinski L. E., Ramírez S. V., Sellgren K., Terndrup D. M., Tiede G. P., 2000, AJ, 119, 536
Evans N. W., 1993, MNRAS, 260, 191
Fanidakis N., Baugh C. M., Benson A. J., Bower R. G., Cole S., Done C., Frenk C. S., Hickox R. C., Lacey C., Del P. Lagos C., 2012, MNRAS, 419, 2797
Förster Schreiber N. M., Genzel R., Bouché N., Cresci G., Davies R., Buschkamp P., Shapiro K., Tacconi L. J., Hicks E. K. S., Genel S., Shapley A. E., Erb D. K., Steidel C. C., Lutz D., Eisenhauer F., 2009, ApJ, 706, 1364
Genzel R., Burkert A., Bouché N., Cresci G., Förster Schreiber N. M., Shapley A., Shapiro K., 2008, ApJ, 687, 59
Goldreich P., Tremaine S., 1979, ApJ, 233, 857
Grosbøl P., Patsis P. A., Pompei E., 2004, A&A, 423, 849
Hernquist L., 1993, ApJ, 409, 548
Hernquist L., Weinberg M. D., 1992, ApJ, 400, 80
Hirschmann M., Naab T., Somerville R. S., Burkert A., Oser L., 2012, MNRAS, 419, 3200
Hohl F., 1971, ApJ, 168, 343
Hohl F., 1976, AJ, 81, 30
Holley-Bockelmann K., Weinberg M., Katz N., 2005, MNRAS, 363, 991

Jenkins A., Binney J., 1990, MNRAS, 245, 305

Jogee S., Barazza F. D., Rix H.-W., Shlosman I., Barden M., Wolf C., Davies J., Heyer I., Beckwith S. V. W., Bell E. F., Borch A., Caldwell J. A. R., 2004, ApJ, 615, L105

Julian W. H., Toomre A., 1966, ApJ, 146, 810

King I. R., 1966, AJ, 71, 64

Kormendy J., Kennicutt Jr. R. C., 2004, ARA&A, 42, 603

Kuijken K., Dubinski J., 1995, MNRAS, 277, 1341

Lelli F., Fraternali F., Sancisi R., 2010, A&A, 516, A11

Lynden-Bell D., 1962, MNRAS, 123, 447

Lynden-Bell D., Kalnajs A. J., 1972, MNRAS, 157, 1

Marinova I., Jogee S., 2007, ApJ, 659, 1176

Matthews L. D., Gallagher III J. S., 1997, AJ, 114, 1899

Mayer L., Wadsley J., 2004, MNRAS, 347, 277

McMillan P. J., Dehnen W., 2007, MNRAS, 378, 541

Menéndez-Delmestre K., Sheth K., Schinnerer E., Jarrett T. H., Scoville N. Z., 2007, ApJ, 657, 790

Miwa T., Noguchi M., 1998, ApJ, 499, 149

Moster B. P., Naab T., White S. D. M., 2013, MNRAS, 428, 3121

Nair P. B., Abraham R. G., 2010, ApJ, 714, L260

Noguchi M., 1987, MNRAS, 228, 635

Ostriker J. P., Peebles P. J. E., 1973, ApJ, 186, 467

Patsis P. A., Skokos C., Athanassoula E., 2002, MNRAS, 337, 578

Pfenniger D., Friedli D., 1991, A&A, 252, 75

Pohlen M., Balcells M., Lütticke R., Dettmar R.-J., 2003, A&A, 409, 485

Polyachenko E. V., 2013, Astronomy Letters, 39, 72

Raha N., Sellwood J. A., James R. A., Kahn F. D., 1991, Nature, 352, 411

Rautiainen P., Salo H., Laurikainen E., 2005, ApJ, 631, L129

Romano-Díaz E., Shlosman I., Heller C., Hoffman Y., 2008, ApJ, 687, L13

Saha K., Gerhard O., 2013, MNRAS, 430, 2039

Saha K., Martinez-Valpuesta I., Gerhard O., 2012, MNRAS, 421, 333

Saha K., Pfenniger D., Taam R. E., 2013, ApJ, 764, 123

Saha K., Tseng Y., Taam R. E., 2010, ApJ, 721, 1878

Sales L. V., Navarro J. F., Theuns T., Schaye J., White S. D. M., Frenk C. S., Crain R. A., Dalla Vecchia C., 2012, MNRAS, 423, 1544

Sellwood J. A., Debattista V. P., 2006, ApJ, 639, 868

Sellwood J. A., Debattista V. P., 2009, MNRAS, 398, 1279

Sellwood J. A., Wilkinson A., 1993, Reports on Progress in Physics, 56, 173

Sheth K., Elmegreen D. M., Elmegreen B. G., Capak P., Abraham R. G., Athanassoula E., Ellis R. S., Mobasher B., Salvato M., Schinnerer E., Scoville N. Z., Spalsbury L., Strubbe L., Carollo M., Rich M., West A. A., 2008, ApJ, 675, 1141

Sheth K., Melbourne J., Elmegreen D. M., Elmegreen B. G., Athanassoula E., Abraham R. G., Weiner B. J., 2012, ApJ, 758, 136

Skokos C., Patsis P. A., Athanassoula E., 2002, MNRAS, 333, 861

Springel V., White S. D. M., Jenkins A., Frenk C. S., Yoshida N., Gao L., Navarro J., Thacker R., Croton D., Helly J., Peacock J. A., Cole S., Thomas P., Couchman H., Evrard A., Colberg J., Pearce F., 2005, Nature, 435, 629

Springel V., Yoshida N., White S. D. M., 2001, NewA, 6, 79

Steinmetz M., Bartelmann M., 1995, MNRAS, 272, 570

Tacconi L. J., Neri R., Genzel R., Combes F., Bolatto A., Cooper M. C., Wuyts S., Bournaud F., Burkert A., Comerford J., Cox P., Davi M., 2012, ArXiv e-prints

Toomre A., 1964, ApJ, 139, 1217

Toomre A., 1981, in S. M. Fall & D. Lynden-Bell ed., Structure and Evolution of Normal Galaxies What amplifies the spirals. pp 111–136

Tremaine S., Weinberg M. D., 1984, MNRAS, 209, 729

Valenzuela O., Klypin A., 2003, MNRAS, 345, 406

Vitvitska M., Klypin A. A., Kravtsov A. V., Wechsler R. H., Primack J. R., Bullock J. S., 2002, ApJ, 581, 799

Weinberg M. D., 1985, MNRAS, 213, 451

Weinberg M. D., Katz N., 2002, ApJ, 580, 627

Weinberg M. D., Katz N., 2007, MNRAS, 375, 425

Yang X., Mo H. J., van den Bosch F. C., Zhang Y., Han J., 2012, ApJ, 752, 41